ACS Catalysis

Research Article

pubs.acs.org/acscatalysis

Mechanism of the Electrocatalytic Oxidation of Formic Acid on Metals

Angel Cuesta,*[,†] Gema Cabello,[†] Masatoshi Osawa,[‡] and Claudio Gutiérrez[†]

[†]Instituto de Química Física "Rocasolano", CSIC, C. Serrano 119, E-28006, Spain

[‡]Catalysis Research Center, Hokkaido University, Sapporo 001-0021, Japan

Supporting Information

ABSTRACT: We present a detailed spectrokinetic study of the electrocatalytic oxidation of formic acid on Au and Pt electrodes using ATR-SEIRAS that has allowed us to unveil the mechanisms of both the direct (in which adsorbed CO is not involved) and the indirect (through adsorbed CO) paths of the reaction with unprecedented detail. Au electrodes were used to study the mechanism of the direct path without the interference of the indirect path, and the observed quadratic dependence of the reaction rate on the formate coverage was then shown to apply also to Pt. The direct path consists of three steps, namely, (i) the electroadsorption of formate (corresponding to the first electron transfer), (ii) the purely chemical bimolecular decomposition of adsorbed formate, and (iii) the second electron transfer. The dehydration of HCOOH to adsorbed CO, that is then oxidized to CO_2 in the indirect path, was studied on Pt at $E < 0.4$ V vs the reversible hydrogen electrode (RHE), at which potentials the dehydration reaction is the only one taking place on the Pt surface. Our results show that adsorbed formate is also the intermediate in the dehydration of formic acid to adsorbed CO and is, hence, the key intermediate in the electrocatalytic oxidation of formic acid on metals.

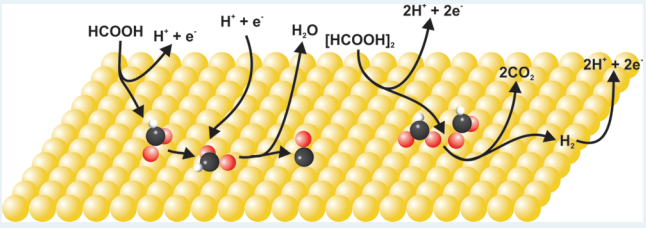

KEYWORDS: *formic acid electrooxidation, Au, Pt, time-resolved ATR-SEIRAS, adsorbed formate, adsorbed carbon monoxide*

1. INTRODUCTION

The electrooxidation of formic acid has attracted the interest of chemists for longer than a century.[1−3] Müller[4] was the first to recognize, back in 1923, that the oxidation of HCOOH on Pt proceeds through two different mechanisms. He was also is the first to detect current oscillations during the electrocatalytic oxidation of formic acid,[5] which he investigated in detail,[6] and related them to the formation of an adsorbed intermediate that blocked the surface, this being probably the first report of what we know today to be the poisoning of the catalyst by adsorbed carbon monoxide formed in the indirect path. The motivation of these early studies was mainly the simplicity of the formic acid molecule, that contains five atoms only, and in which the carbon atom is already bonded to the two oxygen atoms necessary to form CO_2, making it the ideal model for the electrooxidation of oxygenated organic molecules. The interest of this reaction has increased in the past decades, because of the possibility of developing direct formic acid fuel cells (DFACs),[7] that can reach high power densities[8−10] and could be power sources for portable electronic devices.[11]

Despite the extensive and prolonged attention paid to this reaction, the details of its mechanism have remained elusive, the only agreement reached being—back to square one, that is, to the above-mentioned Müller's finding—that the electrooxidation of formic acid on Pt proceeds through a dual-path mechanism,[12,13] composed of a direct path and an indirect path through a poisoning intermediate. On Pt, adsorbed carbon monoxide (CO_{ad}), identified by IR spectroscopy as the poisoning species at the beginning of the 1980s,[14] remained for over 20 years the only adsorbate detected, until Osawa and co-workers demonstrated that bridge-bonded adsorbed formate ($HCOO_{ad}$) is the reactive intermediate in the direct path.[15−20] Very recently,[21] we have demonstrated that, on Pt, $HCOO_{ad}$ is the key intermediate in the electrocatalytic oxidation of formic acid, common to both the direct and the indirect paths, and have shown that, on gold electrodes, the oxidation of $HCOO_{ad}$ to CO_2 proceeds via a chemical bimolecular surface reaction between adjacent $HCOO_{ad}$ species that precedes the second electron transfer.[22] Here, on the basis of both the results reported in refs 21 and 22 and on new experimental evidence, we provide some additional insight into the mechanism of the dehydration of formic acid to adsorbed carbon monoxide on Pt electrodes, and demonstrate that the oxidation of $HCOO_{ad}$ to CO_2 on Pt (and most likely on other transition metals) follows the same mechanism proposed for Au. We believe this to be the first detailed description of the dual-path mechanism of HCOOH electrooxidation.

Special Issue: Electrocatalysis

Received: December 15, 2011
Revised: February 8, 2012
Published: March 19, 2012

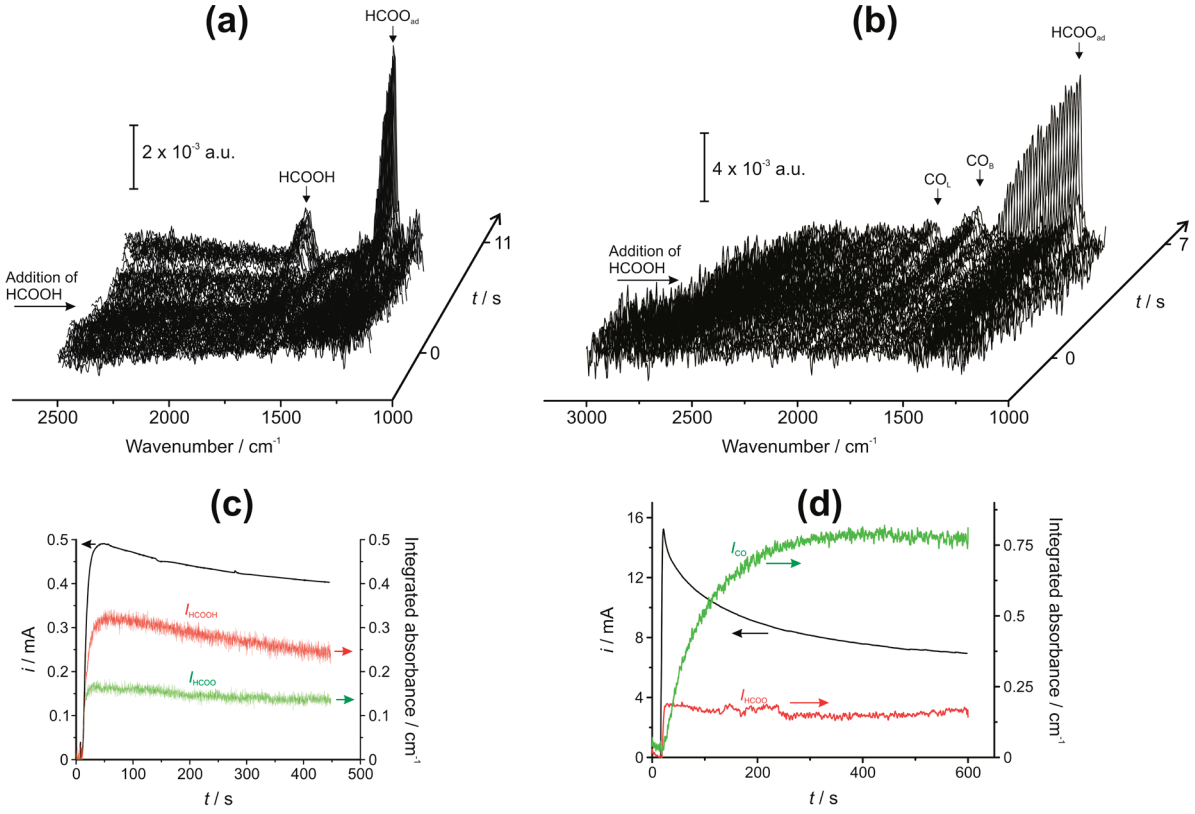

Figure 1. Time-resolved ATR-SEIRA spectra of a gold electrode at 0.76 V (a) and of a platinum electrode at 0.61 V (b) in 0.1 M $HClO_4$ to which the amount of HCOOH necessary to reach a final concentration of 0.1 M was added at the point indicated by the arrow, and corresponding evolution with time of the oxidation current and of the integrated absorbance of the bands observed on gold (c) and on platinum (d). The decrease of the oxidation current after reaching a maximum is due to mass transport limitations. A spectrum recorded at 0.76 V (a) or 0.61 V (b) before the addition of HCOOH was taken as reference. Only the spectra recorded during the first approximately 5 s after addition of HCOOH are shown for the sake of clarity. The time interval between spectra was 140 ms.

2. MATERIALS AND METHODS

The electrode surfaces were monitored during the reaction by surface-enhanced infrared absorption spectroscopy in the Kretschmann ATR configuration (ATR-SEIRAS),[23,24] using a Nicolet 6700 FTIR spectrometer equipped with an MCT detector, and p-polarized light. Each spectrum consisted of a single interferogram, recorded with a spectral resolution of 8 cm^{-1} in the rapid-scan mode, with a time resolution of 140 ms. The differential spectra were calculated as $-\log(R_{sample}/R_{reference})$, where $R_{reference}$ and R_{sample} are the reference and sample spectra, respectively. The working electrodes were either Au or Pt thin films deposited on a Si prism beveled at 60° following previously reported chemical procedures.[15,25,26] A coiled Pt wire and a saturated silver/silver chloride electrode were used as counter and reference electrodes, respectively. All the potentials in the text are referred to the reversible hydrogen electrode (RHE) scale. More experimental details can be found in refs 21 and 22.

We performed the measurements at constant potential, the amount of concentrated HCOOH necessary for reaching the desired final concentration being added just after starting the collection of spectra. With this method data corresponding to all the concentration range of interest can be accrued in a single experiment, since the concentration of formic acid (c_{HCOOH}) at the interface, and therefore the coverage of $HCOO_{ad}$ ($\theta_{formate}$) and, in the case of Pt, of CO_{ad} (θ_{CO}), vary slowly enough as to be followed by time-resolved ATR-SEIRAS. This allows to obtain in a single experiment the dependence of $\theta_{formate}$ on c_{HCOOH}, of the oxidation current (i) on $\theta_{formate}$, and of the rate of CO_{ad} formation on $\theta_{formate}$, to be analyzed.

3. RESULTS

As indicated in ref 22, Au is particularly well suited for studying the mechanism of the direct path of HCOOH electrooxidation, because in acidic media CO does not adsorb on Au, given its low adsorption energy.

In the case of Pt, the mechanism of the direct path can be studied if the contribution of the indirect path to the total current remains negligible or at least constant. As we will show below, this is the case for $E > 0.6$ V. At negative enough potentials ($E \leq 0.45$ V), the current corresponding to HCOOH oxidation on Pt is null or negligible, and the only reaction taking place on the electrode surface is the dehydration of HCOOH to yield CO_{ad}.

3.1. HCOOH Oxidation on Gold and Platinum. Figure 1a shows a series of time-resolved ATR-SEIRA spectra recorded at 0.76 V with Au with an interval of 140 ms following addition of HCOOH to the supporting electrolyte. At the point indicated by the arrow, the volume of concentrated HCOOH necessary to reach a final c_{HCOOH} = 0.1 M was added to the solution. Only the first 4 s after the addition of formic acid are shown for clarity. Only two bands at 1720 and 1329 cm^{-1}, corresponding to HCOOH in the interfacial region and to $HCOO_{ad}$, respectively, emerge in the spectra after addition of HCOOH.

dx.doi.org/10.1021/cs200661z | ACS Catal. 2012, 2, 728–738

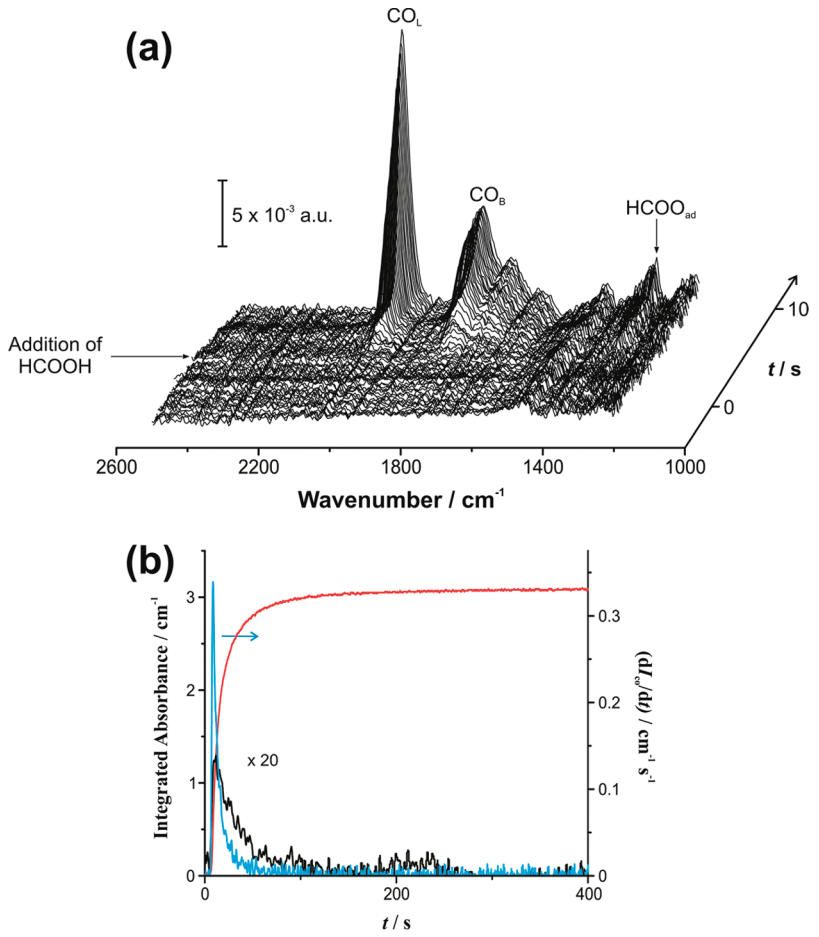

Figure 2. Time-dependent ATR-SEIRA spectra recorded in 0.1 M $HClO_4$ at 0.305 V during the dehydration of formic acid on a thin-film Pt electrode deposited on Si (a) and time dependence of I_{HCOO} (black), I_{CO} (red), and dI_{co}/dt (blue) obtained from them (b). The amount of HCOOH necessary to reach a final concentration of 0.1 M was added at the point indicated by the black arrow. Only the spectra recorded during the first 5 s after addition of HCOOH are shown for the sake of clarity. The time interval between spectra was 140 ms.

A similar experiment with Pt at 0.61 V is shown in Figure 1b. (An experiment with a higher final c_{HCOOH} = 1 M is shown in Supporting Information, Figure S1, together with the corresponding current transient and the time evolution of the integrated intensity of the bands observed.) Two small bands at 1819 and 2028 cm^{-1}, corresponding to bridge-bonded (CO_B) and linearly bonded (CO_L) CO_{ad}, respectively, appear in these spectra at sufficiently long times, in addition to the band at 1326 cm^{-1} typical of $HCOO_{ad}$. The band at 1720 cm^{-1} of bulk HCOOH is absent, indicating that c_{HCOOH} in the some tens of nanometers thick interfacial region probed by ATR-SEIRAS is below the detection limit. Since the bulk c_{HCOOH} is the same in Figures 1a and 1b, this must obviously be due to the much higher activity of Pt toward HCOOH electrooxidation, as compared to Au. Although the diffusion-limited current is not reached, the kinetic current per geometric area is between about 3 and 7 (the roughness factor) times that per real area, so that mass-transport effects are responsible for the continuous decrease of the oxidation current typically found in ATR-SEIRAS experiments, as already noted for both Pt[20] and Au[22] (in the case of Pt, poisoning of the electrode surface by CO_{ad} also contributes significantly to the observed current decay). The higher activity of Pt toward HCOOH electrooxidation is also evident from the small CO_2 band at 2343 cm^{-1} emerging at long enough times (not shown), that was absent in the case of Au.

Figures 1c and d show, for Au and Pt, respectively, the current transients recorded during the experiments and the time evolution of the integrated intensity of the bands observed in the spectra. The integrated intensity of the formic acid band (I_{HCOOH}) is obviously proportional to c_{HCOOH}, the integrated intensity of the formate band (I_{HCOO}) can be assumed to be proportional to $\theta_{formate}$,[20] and the integrated intensity of the CO_L band (I_{CO}) is proportional to θ_{CO} at low θ_{CO}.[27,28]

3.2. Dehydration of HCOOH on Platinum. At negative enough potentials ($E \leq 0.45$ V), the current corresponding to HCOOH oxidation on Pt is null or negligible, and the only reaction taking place on the electrode surface is the dehydration of HCOOH to yield CO_{ad}. Figure 2a shows a series of time-resolved ATR-SEIRA spectra of a Pt electrode in 0.1 M $HClO_4$ recorded at 0.305 V with an interval of 140 ms. At the point indicated by the arrow, the volume of concentrated HCOOH necessary to reach a final concentration of 0.1 M was added to the solution. Only the spectra recorded during the first 5 s after the addition of formic acid are shown for clarity. Figure 2b shows the evolution with time of I_{HCOO} and I_{CO}, and of the time derivative of I_{CO} (dI_{CO}/dt, the rate of formation of CO_{ad}). As reported in ref 21, and as will be shown below, a detailed analysis of the relation between dI_{CO}/dt and I_{HCOO} can provide information of an unprecedented detail on the mechanism of HCOOH dehydration on Pt (and probably on other transition metals).

dx.doi.org/10.1021/cs200661z | ACS Catal. 2012, 2, 728–738

It must be noted that the charge integrated over the necessarily transient process of dehydration of HCOOH to CO_{ad} must be zero, which is perfectly compatible with an initial positive current of HCOOH oxidation to $HCOO_{ad}$ being overlapped and/or followed by a negative current of $HCOO_{ad}$ reduction to CO_{ad}. Therefore, the current measured upon addition of HCOOH at $E \leq 0.4$ V corresponds to the displacement by CO_{ad} of the species initially present at the electrochemical double layer, and is similar to that recorded during a CO charge-displacement experiment (see, e.g., ref 29), carrying very little or no information on the dehydration process.

The dehydration of formic acid to CO_{ad} is a nonredox decomposition reaction, an immediate consequence of which is that neither a reversible potential nor a Tafel slope can be assigned to the global chemical decomposition process. This statement applies to absolutely all nonredox reactions, even if the reaction mechanism can be expressed as a sequence of an electrooxidation followed by an electroreduction (or vice versa), as is the case for the dehydration of HCOOH to CO_{ad}.[21] However, in this case each of the individual electrochemical reactions making up the global chemical decomposition reaction will have a reversible potential and a Tafel slope. It must be therefore clearly specified that these Tafel slopes apply only to the individual electrochemical reactions.

In principle, it is very simple to test if the mechanism of a nonredox decomposition reaction is electrochemical: if there is a wide enough potential range over which only the chemical decomposition occurs, the plot of the reaction rate vs the potential should be of the volcano type, since both anodic and cathodic reactions are involved.

4. DISCUSSION

4.1. The Common Step in the Dual Path Mechanism: Formate Electroadsorption. As we have shown recently,[21] $HCOO_{ad}$ is the point where HCOOH electrooxidation on Pt bifurcates into two separate paths, that is, it is the last intermediate common to both the direct and the indirect pathways. Accordingly, the electroadsorption of formate must constitute the first, common step, in the dual path mechanism.

Au is an ideal electrode for studying the electroadsorption of formate, since this is not accompanied by the adsorption of CO. Figure 3a shows a plot of I_{HCOO} vs I_{HCOOH} at 0.76 and 0.96 V, and Figure 3b shows a Langmuir plot ($1/I_{HCOO}$ vs $1/I_{HCOOH}$) of the same data. The linear relationship between $1/I_{HCOO}$ and $1/I_{HCOOH}$ revealed by Figure 3b suggests that the adsorption of formate can be described by the (completely reversible) Langmuir electroadsorption isotherm, in which the rate of electroadsorption equals the rate of electrodesorption:

$$k_1 \exp\left(\frac{\beta_1 \Delta\varphi F}{RT}\right) c_{HCOOH}(\theta^{max}_{formate} - \theta_{formate}) = k_{-1} \exp\left(\frac{-(1-\beta_1)\Delta\varphi F}{RT}\right)\theta_{formate} \quad (1)$$

where k_1 and k_{-1} are the rate constants of formate electroadsorption and electrodesorption, respectively, β_1 is the anodic symmetry factor and $\Delta\phi$ is the difference between the absolute potential of the electrode and that of the bulk solution. Upon reordering, eq 1 yields:

$$\frac{1}{\theta_{formate}} = \frac{1}{\theta^{max}_{formate}} + \frac{\exp\left(\frac{-\Delta\varphi F}{RT}\right)}{\theta^{max}_{formate} K_L c_{HCOOH}} \quad (2)$$

where $K_L = k_1/k_{-1}$ is the Langmuir constant that would be obtained in the point of zero charge.

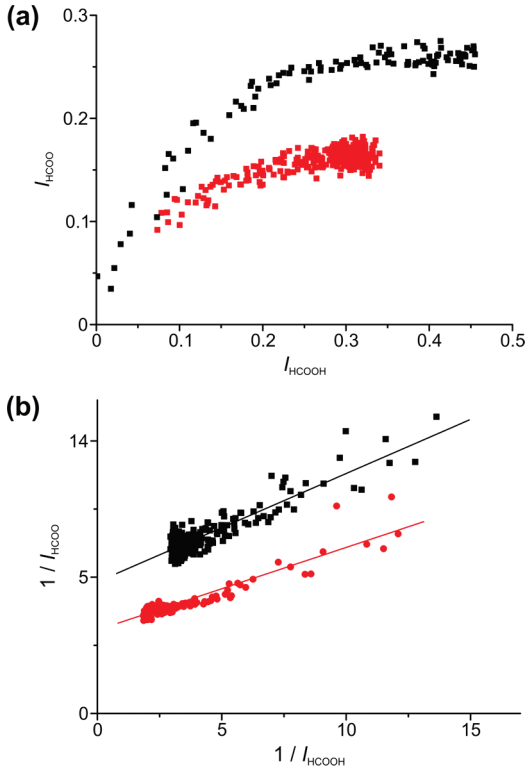

Figure 3. Isotherms (a) and corresponding Langmuir plots (b) for the electroadsorption of formate on Au in 0.1 M $HClO_4$ at 0.76 V (black symbols) and 0.96 V (red symbols).

However, as can be seen in both Figures 3a and 3b, the saturation value depends on the potential, this being a clear indication that the electroadsorption of formate is not in equilibrium. Effectively, for a reversible electroadsorption a decrease of the slope of the Langmuir plot by a factor of 2154 would be expected for a potential increase of 200 mV (a factor of 10 decrease per 60 mV increase), while a decrease by a factor of only 1.3 is observed (Figure 3b). The same dependence of the slope of the Langmuir plot with potential is expected if two formates electroadsorb simultaneously and reversibly from a formic acid dimer, with the simultaneous transfer of the two electrons involved, as we have suggested recently.[22] Actually this same slope is predicted for the simultaneous reversible adsorption of n molecules on n contiguous sites with the simultaneous transfer of the n electrons involved.

Both the potential dependence of the apparent saturation formate coverage and the small decrease of the slope of the Langmuir plots with increasing potential strongly suggest that the electroadsorption of formate on Au is completely irreversible, and that adsorbed formate never desorbs as formic acid, but is further oxidized. In spite of the irreversibility of the adsorption of formate, the concentration dependence of the steady-state $\theta_{formate}$ can still be described by an equation formally identical to the Langmuir isotherm if $HCOO_{ad}$ is

dx.doi.org/10.1021/cs200661z | ACS Catal. 2012, 2, 728–738

oxidized at the same rate at which it is formed. As we have shown recently[22] and will illustrate below, the second step, following the electradsorption of formate, is a purely chemical bimolecular surface reaction between adjacent $HCOO_{ad}$ species. Therefore, the electroadsorption of formate on Au must also be bimolecular, which has led us to suggest that it is a formic acid dimer, not the monomer, the species involved in the reaction.[22] Then, it follows that in the steady state

$$i = k_1 \exp\left(\frac{2\beta_1 \Delta\varphi F}{RT}\right) c^2_{HCOOH}(\theta^{max}_{formate} - \theta_{formate})^2 = k_2 \theta^2_{formate} \quad (3)$$

where k_2 is the rate constant of the chemical step of the oxidation of $HCOO_{ad}$ to CO_2 that precedes the second electron transfer. The factor 2 in the exponential arises because it is assumed that the two electrons involved in the adsorption are transferred simultaneously. Reordering yields the Langmuir-like equation:

$$\frac{1}{\theta_{formate}} = \frac{1}{\theta^{max}_{formate}} + 1 \Big/ \left[\theta^{max}_{formate} \frac{k_1}{k_2} \exp\left(\frac{\beta_1 \Delta\varphi F}{RT}\right) c_{HCOOH}\right] \quad (4)$$

If β_1 has the typically assumed value of 0.5, now a decrease of the slope of the Langmuir plot by a factor of 46.4 would be expected for an increase of the potential of 200 mV (a factor of 10 decrease per 120 mV increase), still clearly larger than the experimentally observed value, this being an indication that $\beta_1 < 0.5$. The same potential dependence of the slope of the Langmuir plot is expected if one formate electroadsorbs irreversibly from a formic acid molecule and is decomposed in a following monomolecular chemical step, and, actually, for the simultaneous irreversible adsorption of n HCOOH molecules on n contiguous sites followed by the decomposition of the n-$HCOO_{ads}$ adsorbate.

A similar spectrokinetic study of the electroadsorption of formate on Pt is complicated by CO poisoning of the electrode surface. Using 0.1 M HCOOH solutions, the band corresponding to bulk HCOOH is only detectable below about 0.6 V and, worse still, overlaps the band of CO_B. We have tried to overcome this difficulty by using a higher concentration, 1 M HCOOH (Supporting Information, Figure S1), but obviously this also increases the rate of formation of CO_{ad}, so that even at potentials as high as 0.81 V I_{HCOO} decreases slowly after reaching a maximum, this being a clear indication of the displacement of $HCOO_{ad}$ from the surface by CO_{ad}. At more positive potentials, oxidation of the surface sets in, introducing additional difficulties.

Fortunately, the electroadsorption of formate on Pt(111) and Pt(554) single-crystal electrodes has been studied by Grozovsky et al. using fast cyclic voltammetry.[30] Since the adsorption and faradaic currents scale with the scan rate and with its square root, respectively, at 50 V s^{-1} the measured current is due exclusively to the rapid electroadsorption-electrodesorption of formate, as clearly shown by the corresponding Nernstian, reversible electroadsorption wave in the cyclic voltammograms.[30] This is confirmed by the about 60 mV slope of a plot of E vs log q_{HCOO} at low q_{HCOO}[31] (where q_{HCOO} is the adsorption charge obtained by integrating the cyclic voltammogram, and is, hence, directly proportional to $\theta_{formate}$), as expected for a completely reversible Langmuir electroadsorption at low coverages. Accordingly, the relation between $\theta_{formate}$ and c_{HCOOH} on Pt can be described by the reversible Langmuir electroadsorption isotherm:

$$\theta_{formate} = \left[\theta^{max}_{formate} K_L \exp\left(\frac{\Delta\varphi F}{RT}\right) c_{HCOOH}\right] \Big/ \left[1 + K_L \exp\left(\frac{\Delta\varphi F}{RT}\right) c_{HCOOH}\right] \quad (5)$$

4.2. Mechanism of the Direct Path: Oxidation of Adsorbed Formate to CO_2. As recently shown,[22] at constant potential, a plot of the current of HCOOH electrooxidation on Au vs the square of the formate coverage (Figure 4a) is linear.

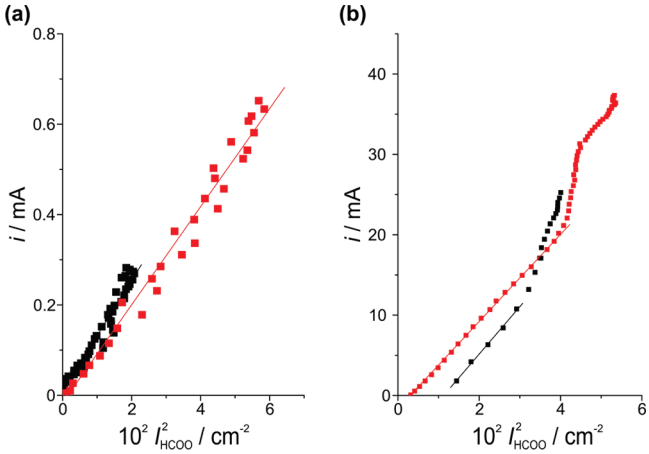

Figure 4. Plots of the HCOOH oxidation current vs the square of the integrated absorbance of the adsorbed formate band. (a) Au electrode at 0.76 V (black symbols) and 0.96 V (red symbols). (b) Pt electrode at 0.61 V (black symbols) and 0.81 V (red symbols).

Moreover, within experimental error, the same current vs $\theta_{formate}$ dependence is obtained at different potentials, that is, the rate at which $HCOO_{ad}$ is oxidized to CO_2 depends exclusively on $\theta_{formate}$. Hence:

$$i = k_2 \theta^2_{formate} \quad (6)$$

As said above, since in the case of Au the dependence of the steady-state $\theta_{formate}$ on the concentration of formic acid can be described by a Langmuir-like isotherm (Figure 3b), the adsorption, which is irreversible, must be bimolecular, since so is the following chemical reaction. The simplest mechanism satisfying these requisites is

$$2HCOOH \rightleftharpoons [HCOOH]_2 + \mathbf{4}^* \rightarrow 2HCOO_{ad} + 2H^+ + 2e \quad (7)$$

$$2HCOO_{ad} \rightarrow 2CO_2 + H_2 + \mathbf{4}^* \quad (8)$$

$$H_2 \rightarrow 2H^+ + 2e \quad (9)$$

It is certainly uncommon for a reaction mechanism to involve the simultaneous adsorption of two identical species. However, in the present case this is well possible, since formic acid in aqueous solutions forms dimers,[32] and it could occur that their adsorption is kinetically favored over that of the monomer.

dx.doi.org/10.1021/cs200661z | ACS Catal. 2012, 2, 728–738

The decomposition of adsorbed formate (Reaction 8) is obviously a redox reaction in which each C atom loses an electron to its adjacent H atom. It involves the rupture of the C−H bond, and therefore would explain the finding of a high kinetic isotope effect for the electrooxidation of HCOOH on Pt.[33,34] Most probably the formation of CO_2 is not accompanied by that of H_{ad}, since formate adsorbs perpendicularly to the metal surface, with the H atom quite distant from it, and the H_2 formed in reaction 8 would be immediately electrooxidized, even on Au, given the high overpotential.

On most metals the reaction with HCOOH gas in UHV produces adsorbed formate,[35−40] which is then either reduced to CO by adsorbed H, with the simultaneous formation of H_2O, or oxidized to CO_2 with the simultaneous formation of H_2.[35−41] The latter has been suggested to occur either by a reaction with adsorbed hydrogen[35] or by a bimolecular reaction between two contiguous adsorbed formates, exactly as in our reaction 8.[35,41]

In the case of Pt, obtaining a correlation between the formic acid oxidation current and $\theta_{formate}$ is only possible if the contribution of the indirect path to the total current remains negligible or constant. These conditions are fulfilled, at least during a short period of time, at $E \geq 0.6$ V.[16,20,42−44] Figure 4b shows plots of the current measured during the electrooxidation of formic acid on Pt vs the square of the formate coverage at 0.61 and 0.81 V. At both potentials the plots are clearly linear during the initial stages of the reaction, when the amount of CO_{ad} accumulated on the surface is very small and therefore the contribution of the indirect path to the total current is negligible. When CO_{ad} starts to accumulate on the surface, the current is even higher than that expected from the quadratic dependence between i and $\theta_{formate}$, clearly indicating a contribution of the indirect path to the total current. This deviation occurs earlier at 0.61 than at 0.81 V, in good agreement with our recent claim that CO_{ad} forms by electroreduction of $HCOO_{ad}$.[21] At 0.81 V, after a slow increase of θ_{CO} and therefore of the contribution of the indirect path to the total current, θ_{CO} remains roughly constant for some time, and the plot of i vs $\theta^2_{formate}$ is again linear, although shifted upward by an amount equivalent to the contribution of the indirect path to i. The quadratic dependence of the reaction rate on the formate coverage is in agreement with the concave shape of the plot of i vs $\theta_{formate}$ reported in refs 20 and 33, and accounts for the observation by Chen et al.[45] that a 10-fold increase of the formic acid concentration multiplies I_{HCOO} by 5, but the current by 20, about the expected value of $5^2 = 25$.

The experimental result that for both Au and Pt the HCOOH oxidation current is proportional to the square of the formate coverage (Figure 4) demonstrates clearly that the mechanism of the direct path of the electrooxidation of HCOOH to CO_2 is essentially the same on Au and Pt electrodes, and very likely also on other noble or transition metals. This mechanism consists of three steps: (i) the electroadsorption of formate, that might be irreversible (Au) or reversible (Pt), this first electron transfer being followed by (ii) the chemical, potential-independent, bimolecular decomposition of two adjacent formates, and, finally, (iii) the second electron transfer, that on both Au and Pt must be much faster than the other two preceding steps, since it does not affect the reaction rate at all. In the case of Pt, since the adsorption of formate is in reversible equilibrium, and so are the monomer and dimer in solution, the monomolecular and bimolecular adsorption of formate are indistinguishable, because they are thermodynamically equivalent.

It is evident from Figure 4 that k_2 is larger for Pt than for Au, since, assuming that the IR absorption coefficient of $HCOO_{ad}$ on Au and Pt is of the same order of magnitude, for a similar formate coverage i is nearly an order of magnitude higher in the case of Pt. Taking into account that, as deduced from Grozovski et al.'s results,[30] the electroadsorption of formate is at equilibrium on Pt, k_1 and k_{-1} must also be larger for Pt than for Au. In summary, Pt has a higher activity for the electrooxidation of formic acid, as compared with Au, because it has higher rate constants both for formate adsorption and for the decomposition of adsorbed formate.

4.2.1. Tafel Slopes of HCOOH Oxidation on Au and Pt. In the case of Au the oxidation of HCOOH to CO_2 begins with the irreversible electroadsorption of two formates on two adjacent sites, and therefore the Tafel slope is obtained already from the equation for the irreversible electroadsorption (eq 3). Accordingly:

$$\frac{\partial \Delta\varphi}{\partial \log i} = \frac{\partial E}{\partial \log i} = 2.3\frac{RT}{2\beta_1 F} \tag{11}$$

Hence, the Tafel slope at low total coverage will be $2.3(RT/2\beta_1 F)$, which for the typically assumed value of $\beta = 0.5$ is 60 mV. We have obtained values between 240 and 270 mV,[22] in excellent agreement with the values of approximately 240 mV obtained by Crépy et al.[46] and by Beltramo et al.[47] These high values of the anodic Tafel slope suggest that β_1 is between 0.125 and 0.11, in good agreement with the conclusion obtained in Section 3.1 from the Langmuir plots in Figure 3b that $\beta_1 < 0.5$. Traditionally, a value of $\beta < 0.5$ has been interpreted as an indication that the transition state resembles more the initial reactant ($[HCOOH]_2$) than its oxidation product ($HCOO_{ad}$), or, equivalently, that the electron transfer occurs closer to the outer Helmholtz plane (OHP) than to the electrode surface. Obviously, at higher $\theta_{formate}$ (i.e., at more positive potentials) the Tafel slope will increase continuously toward infinity with increasing $\theta_{formate}$ (i.e., with increasing potential at constant c_{HCOOH}) as the saturation coverage is approached.

In the case of Pt, for which the electroadsorption of formate is in Langmuir equilibrium,

$$\frac{\theta_{formate}}{\theta^{max}_{formate} - \theta_{formate}} = K'_L \exp\left(\frac{\Delta\varphi F}{RT}\right) c_{HCOOH} \tag{12}$$

where $K'_L = ((k_1/k_{-1})K_{dim})^{1/2}$ is the apparent Langmuir constant at the point of zero total charge.

The current is given by eq 6. Therefore, at low coverages it will be $i = k_2 K_L^2 \exp(2\Delta\phi/RT) c^2_{HCOOH}$, and

$$\frac{\partial \Delta\varphi}{\partial \log i} = \frac{\partial E}{\partial \log i} = 2.3\frac{2RT}{F} \tag{13}$$

and the Tafel slope should be 30 mV. The same Tafel slope would obtain irrespective of the number of formic acid molecules adsorbing reversibly and simultaneously on n contiguous sites and decomposing in a subsequent chemical bimolecular step, since the molecularity of the reversible electroadsorption does not affect eq 12. Again, the Tafel slope will increase continuously toward infinity with increasing $\theta_{formate}$ as the saturation coverage is approached.

Contrary to Au, the determination of the Tafel slope on Pt electrodes is made difficult by the interference of the indirect

dx.doi.org/10.1021/cs200661z | ACS Catal. 2012, 2, 728−738

path. The most recent values of the Tafel slope for the electrooxidation of formic acid on Pt(100), Pt(111) and Pt(110) electrodes (40, 60, and 120 mV, respectively) have been reported by Grozovski et al.,[48] although they were limited to a very narrow potential range of 0.05 V (Pt(100)), 0.1 V (Pt(111)), and 0.15 V (Pt(110)). It is interesting that the highest Tafel slope was found for Pt(110), the surface with the most negative potential of zero total charge, that is, that on which, according to eq 5, the saturation $\theta_{formate}$ will be reached at more negative potentials under otherwise identical conditions.

4.2.2. Acid Test of the Proposed Model, and Obtainment of the Rate Constant of Formate Decomposition, by Conventional Electrochemical Measurements. At constant potential, the current corresponding to the oxidation of formic acid through the reactive pathway will be, in the case of Au,

$$i_{Au} = \left[(\theta^{max}_{formate})^2 k_1 K_{dim} \exp\left(\frac{2\beta_1 \Delta\varphi F}{RT}\right) c^2_{HCOOH} \right] \Big/ \left(1 + \sqrt{\frac{k_1}{k_2} K_{dim}} \exp\left(\frac{\beta_1 \Delta\varphi F}{RT}\right) c_{HCOOH}\right)^2 \quad (14)$$

and, in the case of Pt,

$$i^{direct}_{Pt} = \left[(\theta^{max}_{formate})^2 k_2 {K'_L}^2 \exp\left(\frac{2\Delta\varphi F}{RT}\right) c^2_{HCOOH} \right] \Big/ \left(1 + K'_L \exp\left(\frac{\Delta\varphi F}{RT}\right) c_{HCOOH}\right)^2 \quad (15)$$

Upon reordering

$$\frac{1}{i^{1/2}_{Au}} = \frac{1}{\theta^{max}_{formate} k^{1/2}_{Au}} + 1 \Big/ \left[\theta^{max}_{formate} \sqrt{k_1 K_{dim}} \exp\left(\frac{\beta_1 \Delta\varphi F}{RT}\right) c_{HCOOH} \right] \quad (16)$$

and

$$\frac{1}{(i^{direct}_{Pt})^{1/2}} = \frac{1}{\theta^{max}_{formate} k^{1/2}_2} + 1 \Big/ \left[\theta^{max}_{formate} K'_L \sqrt{k_2} \exp\left(\frac{\Delta\varphi F}{RT}\right) c_{HCOOH} \right] \quad (17)$$

Equations 16 and 17 are extremely important because they allow to confirm or otherwise through conventional electrochemical measurements the mechanism proposed here for the direct path of formic acid electrooxidation. Moreover, from the change with potential of the slope of plots of $1/i^{1/2}$ vs $1/c_{HCOOH}$ at constant potential, it can be checked with a high sensitivity whether formate electroadsorption is in reversible equilibrium or not, since the plot of (log slope) vs potential for reversible electroadsorption should have a slope $1/\beta_1$ times that for irreversible electroadsorption. Most importantly, from the ordinate at the origin the value of k_2, the rate constant of formate decomposition, can be obtained, which allows to compare the activity of different electrode materials.

It has been unequivocally shown that, in the oxidation of HCOOH to CO_2, the intermediate (i.e., $HCOO_{ad}$) is bridge-bonded through its O atoms to no more than two adjacent metal atoms in a bidentate configuration.[49] It is not known yet how the H atom breaks free from $HCOO_{ad}$. Direct C−H bond breaking for the bidentate, upright standing $HCOO_{ad}$ requires a rather high activation barrier >1.2 eV.[50] A slightly lower value, 1.1 eV,[50] has been obtained for a mechanism involving a bi- to monodentate rotation of a solvated $HCOO_{ad}$ for tilting the C−H bond toward the surface (activation energy 0.27 eV[50], 0.7 eV in vacuum, that is, without the solvation effect) followed by the rupture of the tilted C−H bond (activation energy, 0.83 eV[50]). Similar activation energies of 1.2 and 1.1 eV at 0 and 0.5 V have been obtained by Neurock et al.[51] for the C−H bond breaking in $HCOO_{ad}$. They obtained a much lower activation energy, 0.47 eV, for the C−H bond-breaking in $HCOOH_{ad}$ with formation of $COOH_{ad}$,[51] which led them to conclude that $COOH_{ad}$ is the intermediate in the main reaction pathway and $HCOO_{ad}$ is only a site-blocking spectator. However, as we have discussed before,[20] this interpretation is essentially flawed, because, according to Neurock et al., HCOOH converts to $HCOO_{ad}$ spontaneously with a negligible activation barrier, so that $\theta_{HCOOH}/\theta_{formate} = 1.2 \times 10^{-17}$, and this negligible coverage of $HCOOH_{ad}$ cannot contribute significantly to the observed large oxidation current via $COOH_{ad}$. Contrary to Wang and Liu[50] and Neurock et al.,[51] Gao et al.[52] calculated that the activation energy of the formate path (0.73 eV) is slightly lower than that of the direct path via C−H bond breaking in $HCOOH_{ad}$ followed by $COOH_{ad}$ decomposition (0.79 eV). It is evident from this disparity of results that at present a clear conclusion about the mechanism of the electrooxidation of formic acid cannot be reached exclusively from theoretical calculations.

Wang and Liu[50] found that the presence of $HCOO_{ad}$ on the surface favors the adsorption of HCOOH on neighboring sites with the C−H bond directed toward the surface. The activation energy for breaking the C−H bond of adsorbed HCOOH in this configuration is only 0.45 eV, and, consequently, they concluded that the reacting species is this adsorbed HCOOH. However, the mechanism deduced from their density functional theory (DFT) calculations predicts, at low coverage, a linear dependence of the reaction rate on $\theta_{formate}$ (since every $HCOO_{ad}$ would activate a fixed number of neighboring surface sites), which is in contradiction with the experimentally found quadratic dependence.

Therefore, most probably the decomposition of formate (reaction 8) occurs with the two formates remaining in a nearly vertical position, but leaning toward each other until the H atoms break free from the formates and recombine, upon which the remaining OCO species desorb. We believe that this bimolecular reaction provides a feasible route for the rupture of the C−H bond in $HCOO_{ad}$, requiring a lower activation barrier than that of 1.1−1.2 eV calculated by Wang and Liu[50] and Neurock et al.,[51] and even than that of 0.73 eV calculated by Gao et al.,[52] and we expect that theoretical calculations, that have until now never considered such a possibility, will provide additional support to our hypothesis.

However, it has been shown that a full description of the reaction mechanism, including the observation of a maximum in current vs potential plots, requires the introduction in eq 6 of an additional factor, $(1 - \theta)^n$.[16,17,19,20,22,28] We have assigned this factor to the coadsorption of poisoning or spectator species that would reduce the surface area effectively available for the

dx.doi.org/10.1021/cs200661z | ACS Catal. 2012, 2, 728−738

reaction.[22] Alternatively, it could be related to the necessity of free metal atoms adjacent to the couple of reacting adsorbed formates, that would be required for them to rearrange and form the activated complex.

4.3. Formation of the Catalytic Poison on Pt: Reduction of Adsorbed Formate to Adsorbed CO. As shown in Figure 2, at $E \leq 0.45$ V both $HCOO_{ad}$ and CO_{ad} appear immediately on the surface of the Pt electrode after addition of formic acid, but, while the intensity of the CO bands (linear CO (CO_L) and bridge CO (CO_B, not shown)) increases monotonically up to a saturation value, the $HCOO_{ad}$ band increases up to a maximum and then decreases to zero. Moreover, the rate of formation of CO_{ad} is proportional to $\theta_{formate}$ (Figure 5a), and the corresponding proportionality

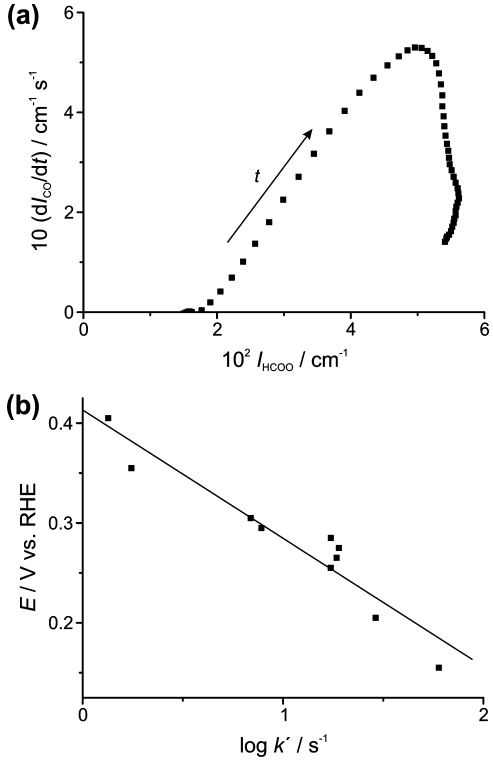

Figure 5. (a) Dependence of the rate of change of the intensity of the band of adsorbed CO, dI_{co}/dt, which is proportional to the rate of formation of adsorbed CO, on the intensity of the band of adsorbed formate, I_{HCOO}, which is proportional to the coverage of adsorbed formate, during the initial stages of the reaction at 0.405 V. (b) Tafel plot of the slope (k') of the plots of dI_{co}/dt vs I_{HCOO}. k' is proportional to k_3, the rate constant for the electroreduction of $HCOO_{ad}$ to CO_{ad} (Reaction 24). A linear fit of the experimental data yields a Tafel slope of −128 mV for this electroreduction. Please note that this Tafel slope has been obtained spectroscopically, and therefore is unaffected by the rate-determining character or otherwise of the step involved.

constant decreases with increasing potential with a slope of −120 mV (Figure 5b). The results in Figure 2 are compatible with three possible mechanisms: (i) chemical dehydration of formic acid followed by displacement of $HCOO_{ad}$ by CO_{ad}; (ii) rate-determining reduction of formic acid followed by rapid oxidation of the resulting species and by displacement of $HCOO_{ad}$ by CO_{ad};[43] and (iii) rapid oxidative electroadsorption of $HCOO_{ad}$ followed by its rate-determining reduction to CO_{ad}.[21] In the following, we will analyze in detail these three mechanisms and their compatibility with the results in Figure 5.

(i) Chemical dehydration of formic acid followed by displacement of $HCOO_{ad}$ by CO_{ad}. In this case, CO_{ad} would form directly from formic acid through a purely chemical dehydration, and $HCOO_{ad}$ would appear on the surface because of its reversible electroadsorption from formic acid, but only transitorily, since it would be displaced by CO_{ad}. The rate of CO_{ad} formation at low CO_{ad} coverage would be

$$\frac{d\theta_{CO}}{dt} = k_{chem} c_{HCOOH} \tag{18}$$

Where k_{chem} is the rate constant of the hypothetical chemical dehydration. Since, as we have shown above, the electroadsorption of formate on Pt can be described by a Langmuir adsorption equilibrium, at low total coverage $\theta_{formate}$ would be given by

$$\theta_{formate} = K_L \exp\left(\frac{\Delta\varphi F}{RT}\right) c_{HCOOH} \tag{19}$$

Therefore

$$\frac{d\theta_{CO}}{dt} = \frac{k_{chem}}{K_L} \exp\left(\frac{-\Delta\varphi F}{RT}\right) \theta_{formate} \tag{20}$$

Accordingly, at constant potential a plot of dI_{CO}/dt vs I_{HCOO} would be linear at low total surface coverage, as in Figure 5a. However, the plot in Figure 5b should have a slope of −60 mV, in contradiction with the value of −120 mV found experimentally.

(ii) Rate-determining electroreduction of adsorbed formic acid followed by rapid oxidation of the resulting reduced species to CO_{ad}, which would then displace $HCOO_{ad}$. This mechanism was proposed by Lu et al.[43] to explain their observation by conventional electrochemical methods that at $E > 0.2$ V the rate of formation of adsorbed CO decreased with increasing potential at the rate of 110 mV per decade. According to them, the first, rate-determining step, would correspond to the electroreduction of adsorbed formic acid to adsorbed $HC(OH)_2$, and the rate of CO_{ad} formation at low total surface coverage would be

$$\frac{d\theta_{CO}}{dt} = k_{Lu} \exp\left(\frac{-(1-\beta_{Lu})\eta_{Lu} F}{RT}\right) K_{Lu} c_{HCOOH} \tag{21}$$

where k_{Lu} is the rate constant for the rate-determining step of the mechanism proposed by Lu et al., β_{Lu} is the corresponding anodic symmetry factor (usually assumed to be 0.5), $\eta_{Lu} = E - E_{eq}$ is the overpotential for the reduction of HCOOH to $HC(OH)_2$, and $K_{Lu}c_{HCOOH}$ is the coverage of adsorbed formic acid at low coverage.

As before, the relation between the formate coverage and the concentration of formic acid will be given, at low total surface coverage, by a Langmuir adsorption equilibrium (eq 19), and the rate of CO_{ad} formation will be:

$$\frac{d\theta_{CO}}{dt} = \frac{k_{Lu}}{K_L} \exp\left(\frac{(-(1-\beta_{Lu})\eta - \Delta\varphi)F}{RT}\right) \theta_{formate} \tag{22}$$

This equation predicts a linear dependence of dI_{CO}/dt on I_{HCOO}, in good agreement with Figure 5a, but, assuming $\beta_{Lu} = 0.5$, it predicts a slope of −40 mV for the plot in Figure 5b, in complete contradiction with the experimentally observed value of −120 mV.

dx.doi.org/10.1021/cs200661z | ACS Catal. 2012, 2, 728−738

(iii) Rapid oxidative electroadsorption of $HCOO_{ad}$ followed by its rate-determining electroreduction to CO_{ad}, which is the mechanism proposed by us.[21] It corresponds to:

$$HCOOH_{aq} \leftrightarrow HCOO_{ad} + H^+ + e^- \quad (23)$$

$$HCOO_{ad} + H^+ + e^- \rightarrow CO_{ad} + H_2O \quad (24)$$

Figure 2 shows that the maximum of the rate of CO formation, dI_{CO}/dt, is reached just before the maximum of I_{HCOO}. Furthermore, dI_{CO}/dt decays much faster than I_{HCOO}, suggesting that the reduction of $HCOO_{ad}$ to CO_{ad} requires adjacent empty sites. Accordingly,

$$\frac{d\theta_{CO}}{dt} = k_3 \exp\left(\frac{-(1-\beta_3)\eta F}{RT}\right)\theta_{formate}(1-\theta_{total}) \quad (25)$$

Where k_3 and β_3 are the rate constant and the anodic symmetry factor, respectively, of Reaction 24 of CO_{ad} formation. At low total surface coverage:

$$\frac{d\theta_{CO}}{dt} = k_3 \exp\left(\frac{-(1-\beta_3)\eta F}{RT}\right)\theta_{formate} \quad (26)$$

Equation 26 is in agreement with the linear dependence of the rate of CO_{ad} formation on $\theta_{formate}$ at low total surface coverage (Figure 5a), and, furthermore, predicts the slope of the plot in Figure 5 b, that in this case corresponds to the Tafel slope of the electroreduction of adsorbed formate to adsorbed CO, to be −120 mV, in perfect agreement with the experimental result.

The mechanism composed of Reactions 23 and 24 is the only one that can explain the results in Figure 5. It is open to confirmation or otherwise by simple experiments, and, furthermore, is supported by recent results of Grozovski et al.[48] They have shown that, for Pt single-crystal electrodes with (111) terraces and (110) steps, the initial rate of dehydration (i.e., that when $\theta_{CO} \rightarrow 0$ and $(1-\theta_{total}) \rightarrow 1$) depends on the electrode potential, showing a symmetric bell shape with a maximum at 0.15 V, the pztc of (110)-oriented sites. They observed the same behavior with Pt single-crystal electrodes with (111) terraces and (100) steps, although in this case the maximum in the dehydration rate appears at around 0.3 V, the pztc of (100)-oriented sites. Assuming that the local $\theta_{formate}$ at the active sites can be described by the Langmuir isotherm for reversible electroadsorption, the initial rate of dehydration will be:

$$\frac{d\theta_{CO}}{dt} = k_3 \exp\left(\frac{-(1-\beta_3)\eta_3 F}{RT}\right)\left[K_L \exp\left(\frac{\Delta\varphi F}{RT}\right)c_{HCOOH}\right] \Big/ \left[1 + K_L \exp\left(\frac{\Delta\varphi F}{RT}\right)c_{HCOOH}\right] \quad (27)$$

Where η_3 is the overpotential for the reduction of asorbed formate to adsorbed carbon monoxide, and $\Delta\phi$ depends on the local pztc of the active site.

Figure 6 shows the potential dependence of the initial rate of HCOOH dehydration predicted by eq 27 for $k_3 = 1\ s^{-1}$, $\beta_3 = 0.5$, $K_L c_{HCOOH} = 0.1$, 1, and 10, and for $\Delta\phi = 0$ V at $\eta_3 = -0.1$, 0, and 0.1 V. As can be seen, the initial rate of dehydration of HCOOH has a symmetric bell shape with a maximum around the pztc, in agreement with the results of Grozovski et al.[48] The maximum shifts to more negative potentials with increasing $K_L c_{HCOOH}$, that is, with increasing concentration of formic acid, and the dehydration rate at the maximum is the higher the more negative is the pztc, this explaining the observation by Grozovski et al.[48] that the activity for the dehydration of HCOOH of Pt(111) is negligible, since its pztc is very positive (0.37 V vs RHE in 0.1 M $HClO_4$[53]). Furthermore, this also explains that, for the same density of steps, Pt single-crystal electrodes with (111) terraces and (100) steps are less active than those with (111) terraces and (110) steps (compare

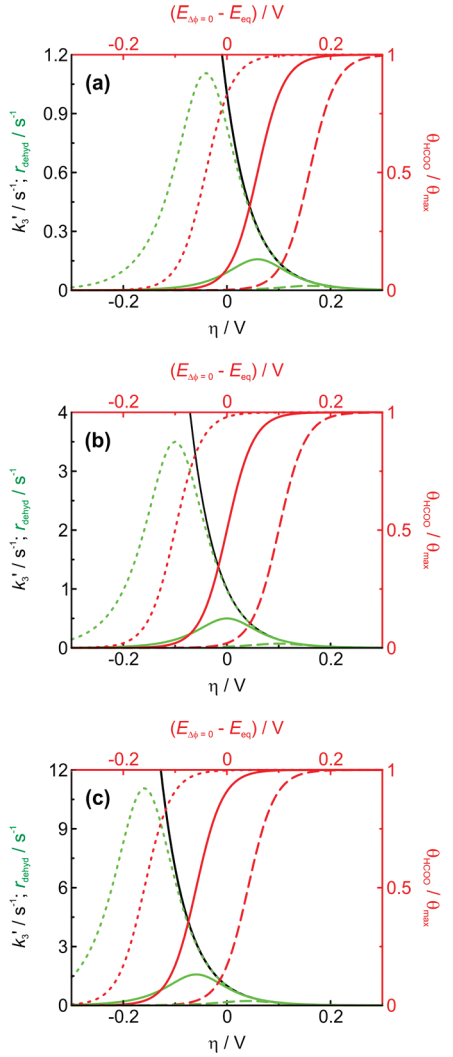

Figure 6. Plot of the rate constant of the reduction of $HCOO_{ad}$ to CO_{ad}, $k_3 \exp(-(1-\beta_3)\eta_3 F)$ (black line), of the formate coverage at Langmuir equilibrium, θ_{HCOO} (red lines), and of their product, which is the rate of dehydration of HCOOH to CO_{ad} (green lines), as a function of potential. The curves have been calculated for $k_3 = 0.1\ s^{-1}$, $K_L = 10$, and $c_{HCOOH} = 1$ M (a), 0.1 M (b), and 0.01 M (c). Three cases have been considered: $\Delta\phi = 0$ at $\eta = -0.1$ V (dotted lines), $\Delta\phi = 0$ at $\eta = 0$ V (solid lines), and $\Delta\phi = 0$ at $\eta = 0.1$ V (dashed lines). It should be noted that only at high enough potentials, at which the saturation formate coverage has been reached, does the rate of the chemical dehydration of HCOOH to adsorbed CO coincide with the rate of the electroreduction of adsorbed formate to adsorbed CO.

dx.doi.org/10.1021/cs200661z | ACS Catal. 2012, 2, 728−738

Figures 7B and 9B in ref 48), even if the activation barrier (i.e., k_3) is the same, because the pztc of (100)-oriented steps is more positive than that of (110)-oriented steps.

It is clearly apparent in Figure 6 that, at positive enough potentials, the rate of CO_{ad} formation coincides with the rate of the electroreduction of adsorbed formate to adsorbed CO. This explains why the value of −110 mV reported by Lu et al.[43] for the potential dependence of the former parameter is in perfect agreement with our observation of a Tafel slope of −120 mV for the latter parameter (Figure 5b).

The potential at which the dehydration rate will be maximum can be found by obtaining the derivative of eq 27 and making it equal to 0. This yields:

$$E_{max} = \left\{2.3\frac{RT}{F}\left[\log\left(\frac{\beta_3}{1-\beta_3}\right) - \frac{1}{2}(\log K'_L)\right] + E_{pzc}\right\} - 2.3\frac{RT}{F}\log c_{HCOOH} \quad (28)$$

according to which a plot of E_{max} vs log c_{HCOOH} must be linear with a slope of −60 mV.

Substituting eq 28 into eq 27 yields an expression for the maximum rate of HCOOH dehydration:

$$r^{max}_{dehyd} = \frac{k_3}{2}\exp\Big\{-(1-\beta_3)\ln\{\beta_3/[(1-\beta_3)\sqrt{K'_L}\,c_{HCOOH}]\} + [-(1-\beta_3)F/RT](E_{pzc}-E_{eq})\Big\} \quad (29)$$

or, in logarithmic form

$$\log r^{max}_{dehyd} = \left\{\log\frac{k_3}{2} - (1-\beta_3)F\left(\frac{(E_{pzc}-E_{eq})}{2.3RT} + [\log\beta_3 - \log(1-\beta_3) - \log\sqrt{K'_L}]\right)\right\} + (1-\beta_3)F\log c_{HCOOH} \quad (30)$$

Equation 30 predicts that, if $\beta_3 = 0.5$ the maximum rate of HCOOH dehydration should increase by a factor of 10 when c_{HCOOH} increases by a factor of 100. It is also evident from eq 30 that, as noted above, the more negative the pzc, the higher r^{max}_{dehyd}, in perfect agreement with the activity sequence (110) > (100) > (111) found by Grozovski et al.[48]

Equations 28 and 30, from which a wealth of kinetic parameters can be obtained, provide a means to check the validity of the dehydration mechanism proposed here, composed of Reactions 23 and 24.

5. CONCLUSIONS

Bridge-bonded adsorbed formate is the most important intermediate in the electrocatalytic oxidation of formic acid on metals, since it is the point where the reaction bifurcates into the direct and indirect pathways, and therefore constitutes the crossroads where it has to be acted if we wish to design an electrocatalyst with a high activity for formic acid oxidation and a low tendency to CO poisoning. In other words, the direct path and the dehydration of formic acid to CO_{ad} must differ only in the transition state, as already suggested 20 years ago by Chang et al.[54] In addition, we have derived equations whose predictions can be checked experimentally, thus providing additional means to check the validity of the statements made here, and from which important kinetic parameters can be determined.

The direct path involves the chemical decomposition reaction between two adjacent adsorbed formates, in principle no adjacent free sites being necessary, while, on the contrary, the dehydration, that involves the electroreduction of one adsorbed formate, requires, at least, one adjacent Pt atom in addition to the two already occupied by $HCOO_{ad}$ (i.e., the smallest atomic ensemble required is a trigonal site[49]). The identification of the transition states will require the concourse of theory.

An important conclusion for which further experimental evidence cannot be obtained, and which therefore will also require the concourse of theory, is our suggestion, based exclusively on the facts that the steady-state formate coverage on Au can be described by a Langmuir-like adsorption isotherm, and that the oxidation current, which in the steady state is necessarily equal to the electroadsorption current, scales with the square of the formate coverage, that the electroadsorption of formate might involve the simultaneous adsorption of two formates from a formic acid dimer.

Finally, the detailed description of the mechanism of the electrooxidation of formic acid on metals provides rational criteria for screening possible electrocatalysts for these important reactions. First of all, the candidate material must have high rate constants for both the electroadsorption and the decomposition of formate, because thus the onset of formate adsorption, and, hence, of formic acid electrooxidation, will tend to approach the reversible potential of HCOOH oxidation. However, this negative shift of the reaction potential will also favor the formation of CO_{ad}, that must be somehow impeded. This might be achieved if the adsorption energy of CO on the candidate material is very low or even positive, like in the case of gold (on which, unfortunately, the electroadsorption of formate is slow), or if k_2, the rate constant for the same-species, bimolecular decomposition of $HCOO_{ad}$ to CO_2 and H_2 is much higher than the rate constant of formate desorption. In the latter case, the electroadsorption of formate will be irreversible and in the stationary state the formate coverage, which will be proportional to $(k_1/k_2)\exp(n\beta_1\Delta\phi/RT)$ will be very low at the low overpotentials of interest for fuel cells, reducing the rate of poisoning by CO_{ad}. This could be the case of Pd, for which $\theta_{formate}$ is very low[55] and which is well known to be poisoned very slowly by CO_{ad}. A third possibility is to take advantage of the different site requirements of the direct and the indirect paths,[49,56] and to engineer the surface of the electrocatalyst, removing from it the sites with three or more contiguous atoms necessary for the reduction of $HCOO_{ad}$ to CO_{ad}.

■ ASSOCIATED CONTENT

Ⓢ Supporting Information

Further details are given in Figure S1. This material is available free of charge via the Internet at http://pubs.acs.org.

■ AUTHOR INFORMATION

Corresponding Author

*E-mail: a.cuesta@iqfr.csic.es. Phone: +34-915619400. Fax: +34-915642431.

Funding

Funding from the DGI (Spanish Ministry of Education and Science) through Projects CTQ2009-07017 and PLE2009-0008 is gratefully acknowledged.

Notes

The authors declare no competing financial interest.

REFERENCES

(1) Bunge, N. A. *Chem. Centralbl.* **1881**, 104.
(2) Jahn, H. *Ann. Phys. Chem.* **1889**, *37*, 408−442.
(3) Salzer, F. *Z. Elektrochem.* **1902**, *8*, 893−903.
(4) Müller, E. *Z. Elektrochem.* **1923**, *29*, 264−274.
(5) Müller, E. *Z. Elektrochem.* **1927**, *33*, 561−568.
(6) Müller, E.; Tanaka, S. *Z. Elektrochem.* **1928**, *34*, 256−264.
(7) Grimes, P. G.; Spengler, H. M. In *Hydrocarbon Fuel Cell Technology*; Baker, B. S., Ed.; Academic Press: New York, 1965, p 121.
(8) Ha, S.; Larsen, R.; Masel, R. I. *J. Power Sources* **2005**, *144*, 28−34.
(9) Zhu, Y.; Khan, Z.; Masel, R. I. *J. Power Sources* **2005**, *139*, 15−20.
(10) Larsen, R.; Ha, S.; Zakzeski, J.; Masel, R. I. *J. Power Sources* **2006**, *157*, 78−84.
(11) Rice, C.; Ha, S.; Masel, R. I.; Waszczuk, P.; Wieckowski, A.; Barnard, T. *J. Power Sources* **2002**, *111*, 83−89.
(12) Breiter, M. *Electrochemical Processes in Fuel Cells*; Springer Verlag: Berlin, Germany, 1969.
(13) Capon, A.; Parsons, R. *J. Electroanal. Chem.* **1973**, *45*, 205−231.
(14) Beden, B.; Bewick, A.; Lamy, C. *J. Electroanal. Chem.* **1983**, *148*, 147−160.
(15) Miki, A.; Ye, S.; Osawa, M. *Chem. Commun.* **2002**, 1500−1501.
(16) Samjeské, G.; Miki, A.; Ye, S.; Yamakata, A.; Mukouyama, Y.; Okamoto, H.; Osawa, M. *J. Phys. Chem. B* **2005**, *109*, 23509−23516.
(17) Samjeské, G.; Osawa, M. *Angew. Chem., Int. Ed.* **2005**, *44*, 5694−5698.
(18) Mukouyama, Y.; Kikuchi, M.; Samjeské, G.; Osawa, M.; Okamoto, H. *J. Phys. Chem. B* **2006**, *110*, 11912−11917.
(19) Samjeské, G.; Miki, A.; Ye, S.; Osawa, M. *J. Phys. Chem. B* **2006**, *110*, 16559−16566.
(20) Osawa, M.; Komatsu, K.-i.; Samjeské, G.; Uchida, T.; Ikeshoji, T.; Cuesta, A.; Gutiérrez, C. *Angew. Chem., Int. Ed.* **2011**, *50*, 1159−1163.
(21) Cuesta, A.; Cabello, G.; Gutierrez, C.; Osawa, M. *Phys. Chem. Chem. Phys.* **2011**, *13*, 20091−20095.
(22) Cuesta, A.; Cabello, G.; Hartl, F.; Escudero-Escribano, M.; Vaz-Domínguez, C.; Kibler, L. A.; Gutiérrez, C.; Osawa, M. *Catal. Today*, submitted for publication.
(23) Osawa, M. *Bull. Chem. Soc. Jpn.* **1997**, *70*, 2861−2880.
(24) Osawa, M. In *Advances in Electrochemical Science and Engineering*; Alkire, R. C., Kolb, D. M., Lipkowski, J., Ross, P. N., Eds.; Wiley-VCH: Weinheim, Germany, 2006; Vol. *9*, pp 269−314.
(25) Miki, A.; Ye, S.; Senzaki, T.; Osawa, M. *J. Electroanal. Chem.* **2004**, *563*, 23−31.
(26) Miyake, H.; Ye, S.; Osawa, M. *Electrochem. Commun.* **2002**, *4*, 973−977.
(27) Heinen, M.; Chen, Y. X.; Jusys, Z.; Behm, R. J. *Electrochim. Acta* **2007**, *52*, 5634−5643.
(28) Samjeské, G.; Komatsu, K.-i.; Osawa, M. *J. Phys. Chem. C* **2009**, *113*, 10222−10228.
(29) Climent, V.; Gómez, R.; Orts, J. M.; Rodes, A.; Aldaz, A.; Feliu, J. M. In *Interfacial Electrochemistry*; Wieckowski, A., Ed.; Marcel Dekker: New York, 1999; p 463.
(30) Grozovski, V.; Vidal-Iglesias, F. J.; Herrero, E.; Feliu, J. M. *ChemPhysChem* **2011**, *12*, 1641−1644.
(31) Herrero, E., *Personal Communication*.
(32) Chmielewska, A.; Wypych-Stasiewicz, A.; Bald, A. *J. Mol. Liq.* **2007**, *130*, 42−47.
(33) Chen, Y. X.; Heinen, M.; Jusys, Z.; Behm, R. J. *Langmuir* **2006**, *22*, 10399−10408.
(34) Chen, Y.-X.; Heinen, M.; Jusys, Z.; Behm, R. J. *ChemPhysChem* **2007**, *8*, 380−385.
(35) Falconer, J. L.; Madix, R. J. *Surf. Sci.* **1974**, *46*, 473−504.
(36) Columbia, M. R.; Crabtree, A. M.; Thiel, P. A. *J. Am. Chem. Soc.* **1992**, *114*, 1231−1237.
(37) Columbia, M. R.; Crabtree, A. M.; Thiel, P. A. *J. Electroanal. Chem.* **1993**, *345*, 93−105.
(38) Columbia, M. R.; Thiel, P. A. *J. Electroanal. Chem.* **1994**, *369*, 1−14.
(39) Bandara, A.; Kubota, J.; Wada, A.; Domen, K.; Hirose, C. *J. Phys. Chem.* **1996**, *100*, 14962−14968.
(40) Huang, J. Y.; Huang, H. G.; Lin, K. Y.; Liu, Q. P.; Sun, Y. M.; Xu, G. Q. *Surf. Sci.* **2004**, *549*, 255−264.
(41) Mars, P.; Scholten, J. J. F.; Zwietering, P. In *Advances in Catalysis*; Frankenburg, W. G., Ed.; Academic Press: New York, 1963; Vol. *14*, pp 35−113.
(42) Clavilier, J. *J. Electroanal. Chem.* **1987**, *236*, 87−94.
(43) Lu, G.-Q.; Crown, A.; Wieckowski, A. *J. Phys. Chem. B* **1999**, *103*, 9700−9711.
(44) Grozovski, V.; Climent, V.; Herrero, E.; Feliu, J. M. *ChemPhysChem* **2009**, *10*, 1922−1926.
(45) Chen, Y. X.; Heinen, M.; Jusys, Z.; Behm, R. J. *Angew. Chem., Int. Ed.* **2006**, *45*, 981−985.
(46) Crépy, G.; Lamy, C.; Maximovitch, S. *J. Electroanal. Chem.* **1974**, *54*, 161−179.
(47) Beltramo, G. L.; Shubina, T. E.; Koper, M. T. M. *ChemPhysChem* **2005**, *6*, 2597−2606.
(48) Grozovski, V.; Climent, V.; Herrero, E.; Feliu, J. M. *Phys. Chem. Chem. Phys.* **2010**, *12*, 8822−8831.
(49) Cuesta, A.; Escudero, M.; Lanova, B.; Baltruschat, H. *Langmuir* **2009**, *25*, 6500−6507.
(50) Wang, H.-F.; Liu, Z.-P. *J. Phys. Chem. C* **2009**, *113*, 17502−17508.
(51) Neurock, M.; Janik, M.; Wieckowski, A. *Faraday Discuss.* **2008**, *140*, 363−378.
(52) Gao, W.; Keith, J. A.; Anton, J.; Jacob, T. *J. Am. Chem. Soc.* **2010**, *132*, 18377−18385.
(53) Cuesta, A. *Surf. Sci.* **2004**, *572*, 11−22.
(54) Chang, S.-C.; Ho, Y.; Weaver, M. J. *Surf. Sci.* **1992**, *265*, 81−94.
(55) Miyake, H.; Okada, T.; Samjeske, G.; Osawa, M. *Phys. Chem. Chem. Phys.* **2008**, *10*, 3662−3669.
(56) Cuesta, A. *ChemPhysChem* **2011**, *12*, 2375−2385.